Bull. Nov. Comp. Center, Num. Model. in Atmosph., etc., 6 (2000), 17–24

Simulation of global atmospheric methane cycle*

V.N. Krupchatnikoff, A.I. Krylova

1. Introduction

In the previous study the three-dimensional climatic model, with realistic representation of global circulation, supplemented by the continuity equation for methane (CH_4) has been considered as a tracer transport model [1]. On the basis of this model there has been performed the simulation of the atmospheric response to the global surface distribution of the background concentration of CH_4 measured in the marine boundary layer at the NOAA/CMDL network for 1984–1987 [2]. Closed contours of maximum concentrations distinguishing geographical source regions and adjacent areas with steep gradients have been derived at the northern mid-latitudes in the atmospheric boundary layer. The main result of the model experiment is that the given transport model allows to interpolate rather sparse ground-based observations derived from 19 sites. Most of the measurement sites are in remote locations, far from methane sources. As atmospheric methane sinks were not included in the model it was possible to interpret the spatial distribution of the methane simulated only within the atmospheric boundary layer.

In this study, the three-dimensional distribution of CH_4 in the atmosphere simulated for the NOAA/CMDL methane data is presented. For the 4-year period (1984–1987) there have been found several features crucial for the global cycle. In the tracer transport model, the main mechanism of the methane destruction in the atmosphere was included. This mechanism is the methane oxidation initialized by reaction with OH radicals in the lower and upper troposphere. The fraction of this methane sink constitutes 0.91 [3]. Stratospheric methane losses and soil absorption takes up less than 10%. Being the dominant path for removal of not only methane but a variety of anthropogenic compounds as well, the OH radical (its global abundance) determines the atmospheric residence times. Since this transport model does not contain the photochemical module with the use of which it could be

*Supported by the Russian Foundation for Basic Research under Grants 00-15-98543, 00-05-65449 and by the Integration Grant 00-76 of SB RAS.

possible to calculate background spatial and temporal distribution of OH in the atmosphere, monthly mean large-scale three-dimensional OH fields taken from [4] are used for computation of chemical destruction of methane in the troposphere.

The introduction of the chemical sink allows to simulate the global atmospheric methane cycle. The essential features of the spatial distribution of CH_4, its annual cycle in the northern hemisphere agree qualitatively with the similar results obtained by Fung et al. [5], by Hein et al. [6] for 1984–1987.

2. Model experiment

The global atmospheric methane cycle was simulated using the tracer transport model [1]. This model includes both photochemical methane losses in the troposphere along with convection which transports CH_4 from the Earth's surface. As a single but the dominant mechanism for removal of CH_4 from the atmosphere the reaction of methane oxidation by OH radical was considered as

$$CH_4 + OH \rightarrow CH_3 + H_2O. \tag{1}$$

This reaction initializes a multistepped transformation of hydrocarbons [7]. Ozone (O_3) molecules and OH radical molecules are formed under the decay of one CH_4 molecule up to final products. The tendencies from the chemical process were calculated as follows:

$$\frac{\partial C}{\partial t} = -LC, \tag{2}$$

where C is a number density (sm^{-3}) for methane, $L = kC_{OH}C_{CH_4}$ is a loss rate (s^{-1}). The rate constant k for reaction (1) according to [8] is taken equal to

$$k = 2.3 \cdot 10^{-12} \cdot \exp(-1700/T)\ sm^3/s.$$

The global background distribution of tropospheric OH within the model year was derived by the interpolation of zonally averaged concentrations for four seasons calculated by the three-dimensional photochemical model of Spivakovsky et al. [4].

The zonally averaged distribution of OH used in the model experiment is shown as a function of latitude and pressure for January, April, July and October in Figure 1. The essential features of the tropospheric OH distribution are the following:

- the decrease of OH concentration with height up to the tropopause (the shape of the vertical distribution of OH reflects the rate of OH production by reaction of the excited oxygen atom with water vapor);

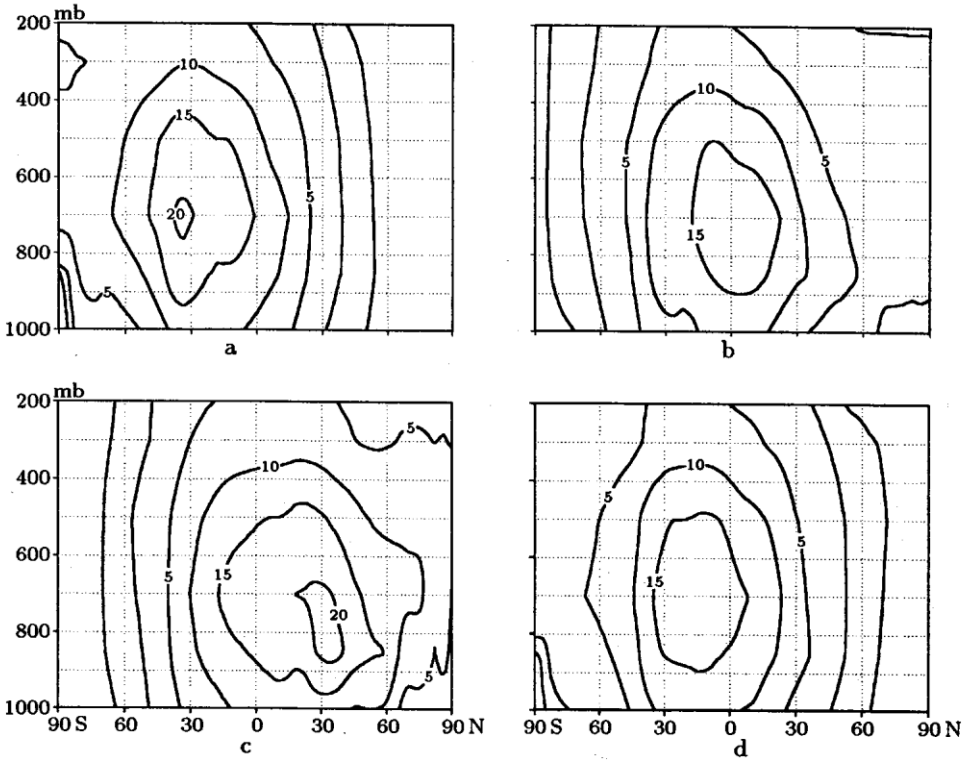

Figure 1. Contours of tropospheric OH (units: 10^5 molecules sm^{-3}) calculated with the three-dimensional model and averaged zonally and monthly for (a) January, (b) April, (c) July, and (d) October. The distribution for tropospheric OH is a function of latitude and pressure (mbar)

- the maximum in the concentration of OH is in the both hemispheres in summer months when the number density of O_3 and solar irradiance peak between 600 and 800 mbar;
- following the sun's seasonal position the concentrations of OH are highest around 30°S in January and 30°N in July.

Tropospheric OH fields exhibit significant seasonal variations in the subtropics, mid-latitudes and subpolar regions. The monthly mean concentrations in excess of 10^6 sm^{-3} extend in the summer hemisphere from the equator to subpolar latitudes while the concentrations in the winter hemisphere are below 10^6 sm^{-3} poleward of 20°.

The simulation of the annual methane cycle was performed for the period of 4 years, starting at a model time of January 1. The period of 1984–1987 is sufficient for finding stable features of atmospheric methane fields: the north-south gradient, seasonal variations. The model experiment was started from a globally uniform background concentration of zero at all

model levels except for the Earth's surface. To analyze seasonal variations the resultant atmospheric concentrations were linearly detrended using the global annually averaged growth rate.

3. The spatial distribution of methane in the troposphere

Figure 2 shows the model distribution of CH_4 derived as an annually averaged for the period of 4 years relative to the global annual mean at the level of 960 mb. Its prominent feature is the north-south gradient with the maximum concentrations of methane in the northern hemisphere. In Northern America closed contours of maximum concentrations which are 90 ppbv larger than the global annual mean are located over the regions, where as it is known there are such continental sources of methane as wetland and landfills. Over Central Europe the highest concentrations of CH_4 ($\sim$ 80 ppbv higher than the global annual mean) occur, where the enteric fermentation of domestic animals, bogs, landfills are the important sources of CH_4. North-eastern regions in Russia referring to the Arctic shows 60–70 ppbv above the global annual mean. They are known to be the regions of clathrate sources. Substantial latitudinal gradients are simulated in the northern and southern tropics indicating the limits of the intertropical convergence zone. According to the model results at the level of 960 mb the latitudinal gradient is determined primarily by the transport, but not by the chemical methane sink. The impact of the hydroxyl OH becomes dominant in the lower and upper troposphere at the tropics. In the northern hemi-

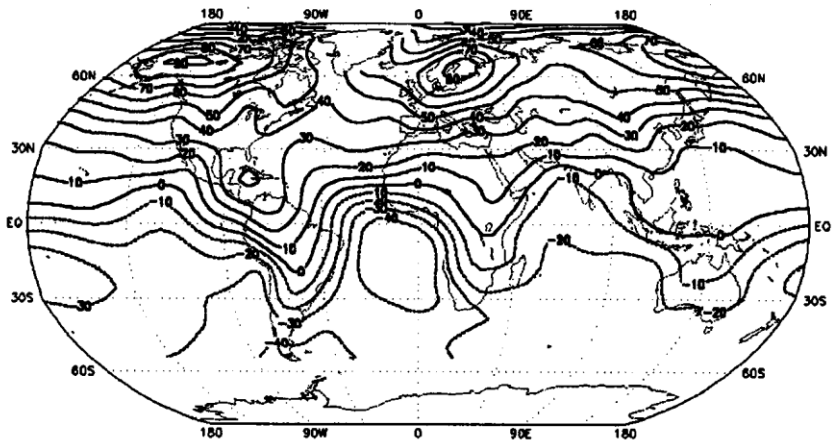

Figure 2. The distribution of the annual mean methane concentration (ppbv – in parts per billion (10^9) by volume in dry air) simulated at 960 mb. Concentrations are defined relative to the global annual mean

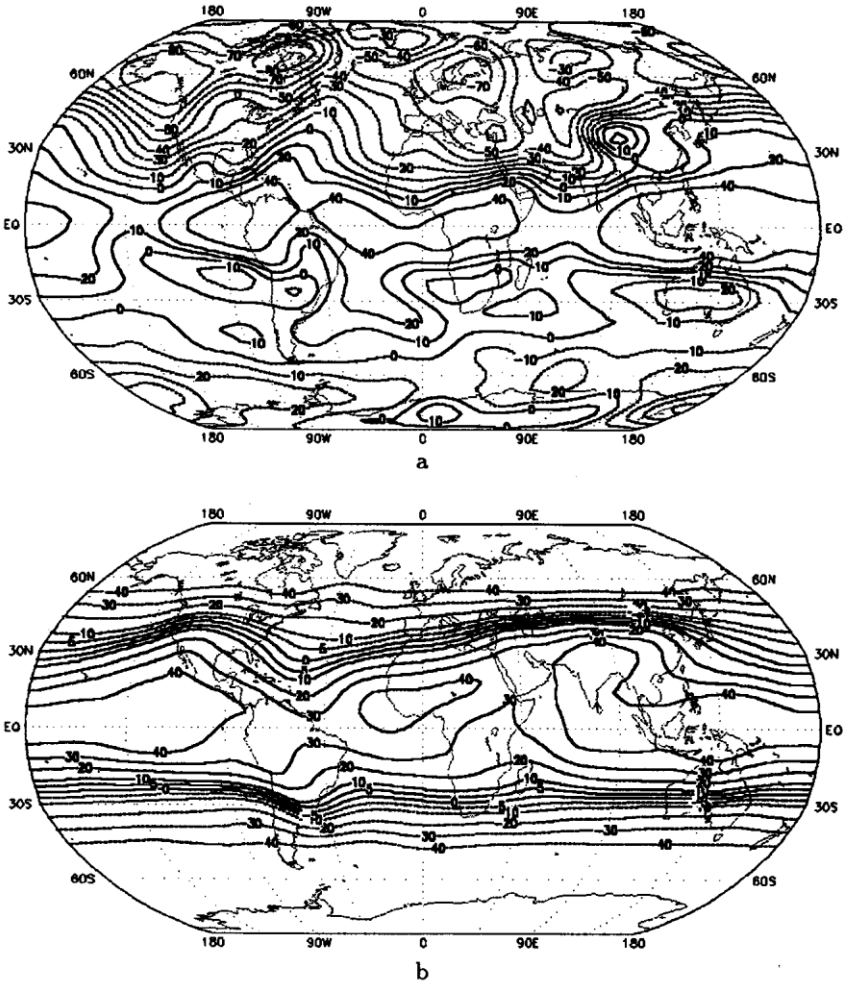

Figure 3. The distribution of the annual mean methane concentration differences (in ppbv units) simulated (a) between ~ 550 and ~ 960 mbar and (b) between ~ 200 and ~ 550 mbar

sphere, near the surface, the concentration of methane over oceanic regions is ~ 30 ppbv lower than over continental sources. Over South America a similar difference in the concentration is found with the surrounding oceans.

The upper panel of Figure 3 represents the difference of the concentrations in the lower troposphere between 550 and 960 mb. According to the model results in the northern hemisphere the concentration declines with height both over the land and the ocean, and in the southern hemisphere over the continental regions. In these regions, emission from the surface advected and convected by the circulation dominates over the chemical distraction in the determination of the vertical profile. Closed contours of the negative

difference in the concentration (the smallest difference of ~ -80 ppbv) indicate distinctly the location of the main continental methane sources. To some extent the model results may be considered as a solution of an inverse problem in which the location of emission methane sources is defined from observed concentrations at a sparse network of sites. In the southern hemisphere over oceans in the lower troposphere the positive vertical gradient is formed. It can be explained by the fact that signals advected longitudinally from continental sources and latitudinally from the northern hemisphere are weak as compared to the chemical sink. In this layer, methane increases with height by 10–40 ppbv.

For the upper troposphere (between 200 and 550 mb) the sign of the methane vertical gradient is mainly similar to that of the lower troposphere (the lower panel of Figure 3). Over the continental regions of the southern hemisphere, however, the gradient changes its sign. The vertical gradient is mainly defined by methane sources over these regions in the lower troposphere while in the upper troposphere the chemical sink is largely responsible for the vertical gradient of CH_4. Above 500 mb methane is almost homogeneously mixed meridionally and the chemical sink is the dominant mechanism forming the vertical profile of the concentration.

In the northern hemisphere for the level of 960 mb a model seasonal cycle is characterized by the complex double fall-winter maximum (Figure 4). Emissions from wetland which reach their maximum in September generate the first maximum in October. This model maximum appears a month early than in the observed data. Methane oxidation by the hydroxyl OH is weak in winter. The double maximum in seasonal variations is due to the increase of emissions in fall and the decrease of the sink during winter.

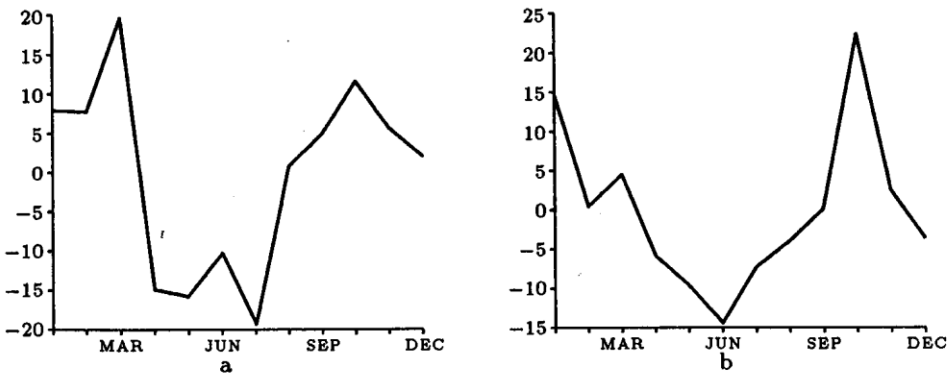

Figure 4. Seasonal cycle of atmospheric methane concentration (in ppbv units) in the northern hemisphere at 960 mb for (a) Mould Bay (76°N) and (b) Byelorussia (53°N). For each location, the average long-term trend has been subtracted from concentrations simulated

The minimum in the seasonal variations of CH_4 found in summer can be primarily explained by the maximum sink of methane as the concentrations of the hydroxyl OH radical peak in summer. Besides the impact of this mechanism, apparently, it is necessary to consider the fact that air fluxes in the tropics transported by the lower division of the Hadley cell in spring is much larger than the fluxes via the troposphere. The increased transport of methane in the tropics during spring definitely contributes to the minimum of CH_4 which is simulated at the surface of 960 mb in June–July.

As it has been shown earlier in the southern hemisphere the distribution of CH_4 is defined to a considerable extent by the tropospheric distribution of OH. Due to smaller amplitudes of OH variations as compared to the northern hemisphere the seasonal cycle of CH_4 in this hemisphere is rather weak.

4. Conclusions

On the basis the global transport model, the methane data measured in the marine boundary layer for 1984–1987 and three-dimensional fields of the hydroxyl OH the spatial and temporal distribution of CH_4 in the atmosphere has been simulated. To study chemical reactive tracers the realistic climatic model of the atmospheric dynamics was used as a global transport model complemented by the continuity equation of methane [1]. The obtained results evidence for the ability of the given model to reproduce the global atmospheric methane cycle and to simulate real seasonal variations. The model results agree qualitatively with those reported by several authors [5, 6] for the period of 1984–1987 and emphasize the sufficiency of a 4-year period to establish prominent features of the distribution of methane in the atmosphere.

References

[1] Krupchatnikoff V.N., Krylova A.I. Numerical simulation of methane distribution using data of ground-based observations // Atmospheric and oceanic optics. – 2000. – № 6–7. – P. 622–626.

[2] Trends'93: A Compendium of Data on Global Change / Ed.: M.A. Boden, D.P. Kaiser, R.J. Sepansky, F.W. Stoss. – Tennessee, 1994.

[3] Aselmann J., Crutzen P.J. Global distribution of Natural Freshwater Wetlands and Rice Paddies, their not primary productivity, seasonality and possible methane emissions // J. Atmos. Chem. – 1980. – Vol. 8. – P. 307–358.

[4] Spivakovsky C.M., Yevich R., Logan J.A. et al. Troposphere OH in 3-dimensional tracer model, an assessment based on observations of CH_3CCl_3 // J. Geoph. Res. – 1990. – V. 95, № D11. – P. 18441–18471.

[5] Fung I., John J., Lerner J. et al. 3-dimensional model synthesis of the global methane cycle // J. Geoph. Res. – 1991. – № D7. – P. 13033–13065.

[6] Hein R., Crutzen P.J., Heimann M. An inverse modeling approach to investigate the global atmosphere methane cycle // Global Biogeochemical Cycles. – 1997. – Vol. 11, № 1. – P.43–76.

[7] Bazhin N.M. Sources and sinks of atmospheric methane // Chemistry for Sustainable Development. – 1993. – Vol. 1. – P. 331–346.

[8] DeMore W.B., Molina M.J., Sander S.P. et al. Chemical kinetics and photochemical data for use in atmospheric modelling // JPL Publ. – 1987. – P. 87–91.